

Constraining Sea Quark Distributions Through W^\pm Cross Section Ratios Measured at STAR

M. Posik* (for the STAR Collaboration)

Temple University, Philadelphia, PA, USA

E-mail: posik@temple.edu

Over the past several years the STAR experiment at RHIC has been contributing to our understanding of the proton structure. Through its instrumentation, STAR is well equipped to measure $W \rightarrow \nu + e$ in $\sqrt{s} = 500/510$ GeV proton-proton collisions at mid-rapidity ($-1.1 \leq \eta \leq 1.1$). The W cross section ratio (W^+/W^-) is sensitive to unpolarized u , d , \bar{u} , and \bar{d} quark distributions. At these kinematics, STAR is able to measure the quark distributions near Bjorken- x values of 0.1. The RHIC runs in 2011, 2012 and 2013 at $\sqrt{s} = 500/510$ GeV saw a significant increase in delivered luminosity from previous years. This resulted in a total data sample being collected of about 352 pb^{-1} of integrated luminosity. The increased statistics will lead to a higher precision measurement of the W^+/W^- cross section ratio than was previously measured by STAR's 2009 run, as well as allow for a measurement of its η dependence at mid-rapidity. Presented here is an update of the W cross section ratio analysis from the STAR 2011, 2012 and 2013 runs.

The XXIII International Workshop on Deep Inelastic Scattering and Related Subjects

April 27 - May 1, 2015

Southern Methodist University

Dallas, Texas 75275

*Speaker.

1. Motivation

Over the past several years parton distribution functions (PDFs) have been becoming more and more precise [1, 2, 3]. However, there are still regions in which more precision data is needed which can be used to help constrain the PDFs. For example the sea quark distributions near the valence region, $x \sim 0.1-0.3$, still have sizable uncertainties [4].

One of the data sets used to determine the anti-quark PDFs is the \bar{d}/\bar{u} measurement from E866 [5], which measured \bar{d}/\bar{u} to good precision at lower x ($x < 0.15$). However, their precision quickly deteriorates as they approach higher x ($x > 0.2$). These data suggest an interesting behavior, as x increases there seems to be a transition from being \bar{d} dominated to \bar{u} dominated around $x \sim 0.25$. Many models are able to describe the general $\bar{d} > \bar{u}$ behavior seen at low x , but fail to predict the suggested $\bar{u} > \bar{d}$ transition [6]. To better determine the behavior of \bar{d}/\bar{u} the experiment SeaQuest (E-906) [7] has been designed and is currently running. Through Drell-Yan scattering, SeaQuest will probe the sea quark distribution at lower Q^2 than E866, but increase the precision and x reach of the \bar{d}/\bar{u} measurement. Although this will help constrain the PDF fits, ideally one would like more data to fit from different scattering processes and Q^2 scales. This will help to add more independent data to global fits, and serve as a cross check of our understanding of the QCD sea.

The W boson production in proton-proton collisions is also sensitive to the sea quarks. The W^+ boson is sensitive to the \bar{d} quark, while the W^- boson is sensitive to the \bar{u} quarks which can be seen in equation 1.1, and probes the distribution at $Q^2 \sim M_W^2$. The leptonic decay from W bosons can be detected by looking for leptons with a high transverse momentum, p_T , near $M_W/2$. Then a charge separation of the leptons can be used to determine which charged W boson they decayed from.

$$u + \bar{d} \rightarrow W^+ \rightarrow e^+ + \bar{\nu}, \quad d + \bar{u} \rightarrow W^- \rightarrow e^- + \bar{\nu}. \quad (1.1)$$

By considering the leading order expression for the charged W cross section ratio [8], $\frac{\sigma_{W^+}}{\sigma_{W^-}}$ (R_W), the direct relationship to the sea quarks can be seen

$$R_W \equiv \frac{\sigma_{W^+}}{\sigma_{W^-}} \sim \frac{u(x_1)\bar{d}(x_2) + \bar{d}(x_1)u(x_2)}{\bar{u}(x_1)d(x_2) + d(x_1)\bar{u}(x_2)}. \quad (1.2)$$

It should be noted that although R_W can be measured at the LHC, the region of x that would be probed is below the valence region near $x \sim 0.08$ (assuming a $\sqrt{s} = 1$ TeV and $\eta = 0$).

2. Experiment

The STAR experiment at RHIC [9] serves as an excellent place to measure the charged W cross section ratio, which was first measured in the STAR 2009 run [10]. The STAR experiment measured R_W using proton-proton collisions at center of mass energies of $\sqrt{s} = 500/510$ GeV in the mid-rapidity region ($-1.1 \leq \eta \leq 1.1$). Several sub-detectors were used to select the W events and separate their charge: the time projection chamber (TPC) [11], used for particle tracking, and the barrel electromagnetic calorimeter (BEMC) [12], used to measure particle energy. A third

sub-detector, the endcap electromagnetic calorimeter (EEMC) [13], was used to estimate the background contributions. The mid-rapidity region of STAR corresponds to about $0.1 \leq x \leq 0.3$ and $Q^2 \sim M_W^2$, which could have an impact on constraining PDFs as this is the x region where E866's precision starts to drop off and is the region where the data suggests that the \bar{u} quark density is greater than the \bar{d} quark density. STAR has taken advantage of the yearly increase in luminosity that RHIC has provided. This luminosity increase has led to roughly 352 pb^{-1} of integrated luminosity being collected during the 2011-2013 runs. With the 2013 data set still under analysis, a preliminary R_W result is presented using only a fraction (102 pb^{-1}) of the collected 2011-2013 data.

3. Results

The leptons from W decay are selected by following the methodology previously established by STAR [10]. Several cuts which include matching high p_T tracks to BEMC clusters, a series of isolation cuts used to isolate the leptons, a p_T -balance cut which looks for the large missing neutrino momentum, and a charge separation cut are applied to select leptons that are likely produced from W decay. Figure 1 shows the application of several isolation cuts and charge separation cuts to the data. In panel a), one can see that as more isolation cuts are applied there is a decrease in background events, which populate the kinematic region $E_T < 25 \text{ GeV}$, and an enhancement of the lepton signal near $E_T \sim M_W/2$. Panels b) and c) show cuts applied to the data in order to select events which have likely originated from W^+ or W^- decays. Panel b) shows the charge separation as a function of E_T , while panel c) projects the charge separation as a function of E_T on to the charge separation axis. The charge separation cuts are indicated by the red lines and were chosen to avoid contamination from the opposite charge.

The charged W cross section ratio can be measured experimentally as

$$\frac{\sigma_{W^+}}{\sigma_{W^-}} = \frac{(N_O^+ - N_B^+) \varepsilon^-}{(N_O^- - N_B^-) \varepsilon^+}, \quad (3.1)$$

where \pm corresponds to positively or negatively charged lepton, N_O are the number of events that pass the lepton selection cuts, N_B are the number of background events estimated to be contaminating the data set, and ε is the efficiency at which W events are detected.

Figure 2 shows the various background contributions, Monte Carlo simulation of the W decay (based on Pythia 6.4.22 [14] and GEANT [15]), and a comparison of the data to Monte Carlo W signal with background contributions included for the 2011 and 2012 data sets. The background contribution labeled *Second End Cap* is an estimate of the background caused by an escaping jet's p_T being misidentified as the neutrino's missing p_T . This is predominately a QCD like background. When the final cut of $E_T > 25 \text{ GeV}$ is applied, there is very little background contributions from $W \rightarrow \tau + \nu$ and $Z \rightarrow ee$ decays. The background was found to be dominated by QCD background.

A Monte Carlo based on Pythia 6.4.22 [14] and GEANT [15] is used to determine the W^\pm detection efficiencies, shown in Fig. 3. These efficiencies account for all cut and detector efficiencies. The 2011 data was found to have a higher efficiency than the 2012 data due to running at a higher luminosity rate in 2012. Running at a higher instantaneous luminosity lead to more pile-up in the TPC, which resulted in less efficient track reconstruction and hence less efficient W detection.

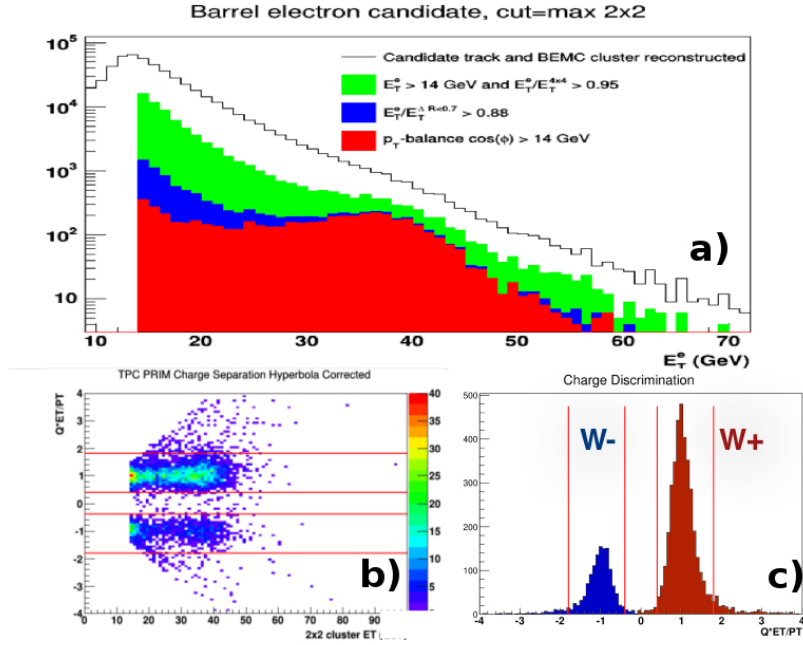


Figure 1: Some cuts applied to data used to select leptons which likely originated from W decay. a) Application of several isolation cuts including a minimum E_T cut, electron energy ratio cuts, and a signed p_T cut. b) Charge separation cut vs. E_T . c) Projection of the charge separation vs. E_T projected onto the charge separation axis.

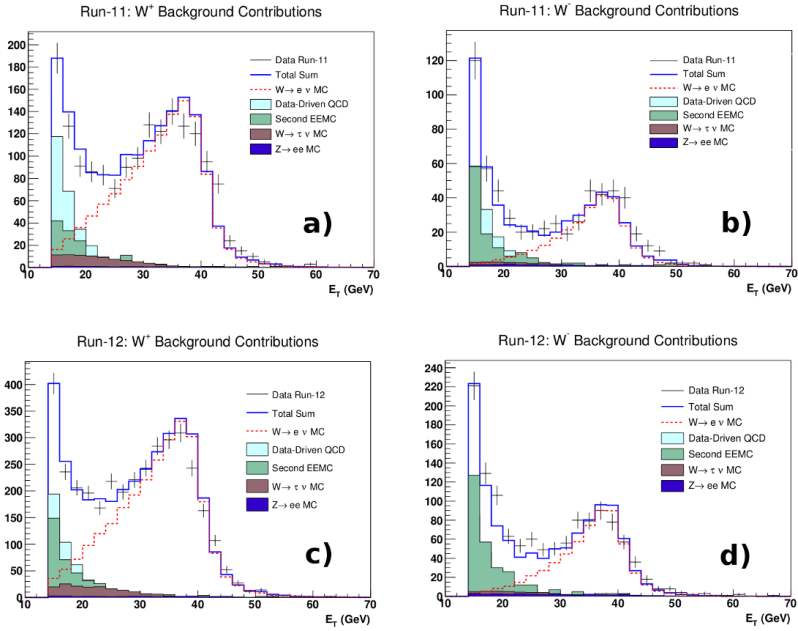


Figure 2: Background and Monte Carlo contributions compared to data. a) Run-11 W^+ , b) Run-11 W^- , c) Run-12 W^+ , and d) Run-12 W^- .

However in both data sets there was only a small (~ 1 -2%) charge dependence measured between the W^+ and W^- efficiencies, which means the $\frac{\epsilon^-}{\epsilon^+}$ factor will have a negligible contribution to the charged W cross section ratio.

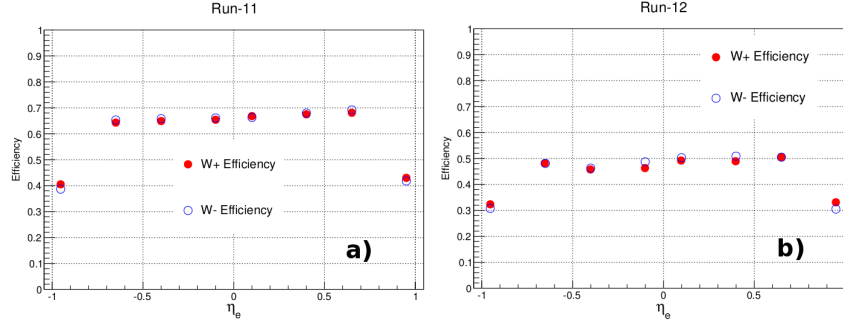


Figure 3: W^+ and W^- efficiencies as a function of electron pseudo-rapidity for a) Run-11 and b) Run-12.

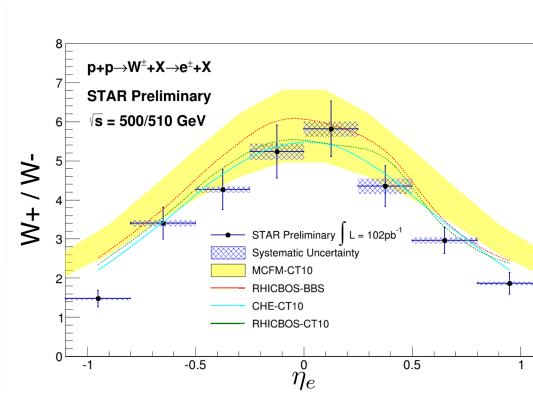


Figure 4: W^+/W^- cross section ratio as a function of electron pseudo-rapidity.

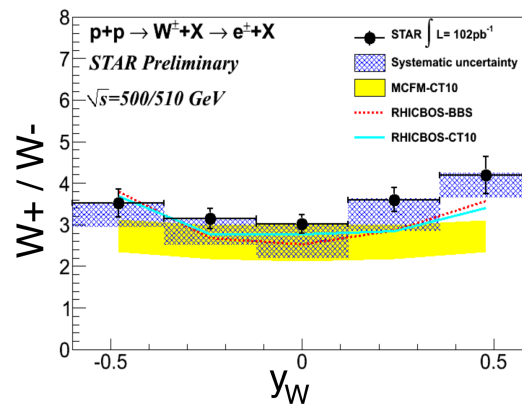


Figure 5: W^+/W^- cross section ratio as a function of the W boson rapidity.

Figure 4(5) shows the charged W cross section ratio for the combined 2011 and 2012 runs, computed using equation 3.1, as a function of the electron pseudo-rapidity, η_e (W boson rapidity,

y_W). More information on how the W boson kinematics were reconstructed can be found in [16, 17]. The error bar on the data points represents the statistical uncertainty, while the shaded boxes correspond to the systematic uncertainty. The yellow band and colored curves serve as a comparison to different PDF sets [18, 19] and theory frame works [20, 21]. Note that the systematic uncertainties for the charged W cross section ratios as a function of η_e are well under control and we are dominated by our statistical precision. Further studies into the newly established W boson reconstruction process [16, 17] should reduce the systematic uncertainties on the W^\pm cross-section ratio dependence on the boson kinematics.

4. Summary

We have measured and presented charged W cross section ratios from combined 2011 and 2012 proton-proton STAR data at $\sqrt{s} = 500/510$ GeV. The inclusion of this data into global PDF analysis should help constrain the sea quark distributions and provide additional insight into the \bar{d}/\bar{u} ratio near the valance region. Furthermore, with the inclusion of the STAR 2013 data (~ 250 pb $^{-1}$), we will be able to further improve on the precision of our charged W cross section ratios.

References

- [1] J. Gao *et al.*, Phys. Rev. D, **89**, 3, 033009 (2014).
- [2] S. Alekhin, *et al.*, arXiv:1410.4412 [hep-ph] (2015).
- [3] R. D. Ball, *et al.*, The NNPDF Collaboration, arXiv:1410.8849 [hep-ph] (2015).
- [4] J. Gao and P. Nadolsky, JHEP, **1407**, 035 (2014).
- [5] R. S. Towell *et al.*, Phys. Rev. D, **64**, 052002 (2001).
- [6] Wen-Chen Chang and Jen-Chieh Peng, *Progress in Particle and Nuclear Physics*, **79**, 95(2014).
- [7] P. E. Reimer (SeaQuest), J. Phys. Conf. Ser. **295**, 012011 (2011).
- [8] C. Bourrely and J. Soffer, Nucl. Phys. B **423**, 329 (1994).
J. Soffer, C. Bourrely, and F. Buccella, arXiv:1402.0514 (2014).
- [9] K. H. Ackermann *et al.* (STAR), Nucl. Instrum. Meth. **A 499**, 624 (2003).
- [10] L. Adamczyk *et al.* (STAR), Phys. Rev. D **85**, 092010 (2012).
- [11] M. Anderson *et al.* (STAR), Nucl. Instrum. Meth. **A 499**, 659 (2003).
- [12] M. Beddo *et al.* (STAR), Nucl. Instrum. Meth. **A 499**, 725 (2003).
- [13] C. Allgower *et al.* (STAR), Nucl. Instrum. Meth. **A 499**, 740 (2003).
- [14] T. Sjostrand, S. Mrenna, and P. Skands, *Pythia 6*, <https://pythia6.hepforge.org>.
- [15] S. Agostinelli *et al.*, Nucl. Instrum. Meth. **A 506**, 250 (2003).
- [16] S. Fazio and D. Smirnov (STAR), PoS, DIS2014, 237, (2014).
- [17] S. Fazio (STAR), These Proceedings (2015).
- [18] H. L. Lai *et al.*, Phys. Rev. D, **82**, 074024 (2010).

- [19] C. Bourrely, F. Buccella, and J. Soffer, *Eur. Phys. J. C* **23**, 487 (2002).
- [20] J. Campbell, K. Ellis, and C. Williams, *MCFM - Monte Carlo for FeMtobarn Processes*, mcfm.fnal.gov.
- [21] P.M. Nadolsky and C.-P. Yuan, *Nucl. Phys. B* **666**, 3 (2003).